

RESEARCH ARTICLE

Optimal sensor placement for modal parameter identification of steeltimber composite beams

Fezayil Sunca^{1,2*}

- ¹ Karadeniz Technical University, Earthquake and Structural Health Monitoring Research Center, Trabzon, 61080, Türkiye
- ² Karadeniz Technical University, Department of Construction Technologies, Trabzon 61080, Türkiye

Article History

Received 14 July 2025 Accepted 22 September 2025

Keywords

Ambient vibration test
Effective independence method
Modal parameters
Optimal sensor placement
Steel-timber composite beam

Abstract

In vibration tests, the number and placement of sensors play a critical role in ensuring the quality of vibration signals and the reliability of identified modal parameters. For effective structural identification, it is essential to select sensor locations that enable accurate tracking of structural behavior with minimal instrumentation. In this study, the applicability and effectiveness of optimal sensor placement for identifying modal parameters of a steel-timber composite beam using ambient vibration tests were investigated. To this aim, a beam was constructed under laboratory conditions, and vibration tests were performed to determine its modal parameters. Initially, ambient vibration tests of the beam were performed using a large number of accelerometers. Subsequently, the optimal sensor layout was determined using the Effective Independence method, and the vibration tests were repeated accordingly. Experimental modal parameters were extracted using the Enhanced Frequency Domain Decomposition method. A comparative analysis revealed that the EFI-based optimal sensor configuration effectively captured the key modal parameters with fewer sensors, thereby maintaining reliability and accuracy. This demonstrated that optimal sensor placement could significantly reduce instrumentation without compromising the quality of identification.

1. Introduction

The modal parameters are key factors that identify the structural behavior of engineering structures. These parameters (natural frequency, damping ratio, and mode shape) are typically determined through modal analyses performed with finite element (FE) models during the design phase of the relevant structure. However, discrepancies often arise between the analytically estimated and the actual dynamic responses observed in the as-built structure due to several reasons, including construction imperfections, material deterioration, and alterations in boundary conditions. Consequently, it is important to verify the numerical modal parameters through vibration tests that accurately represent the in-situ condition of the structure [1,2]. For this purpose, several studies have evaluated the vibration-based behavior of many engineering structures such as bridges [3-5], dams [6,7], and buildings [8,9]. In addition, load-bearing elements such as timber-based composites have become important research topics in recent years. Wang et al. [10] investigated the

eISSN 2630-5763 © 2025 Authors. Publishing services by golden light publishing®.

^{*} Corresponding author (<u>fezayilsunca@ktu.edu.tr</u>)

dynamic modulus of elasticity and the damping ratio of timber-based composites using the cantilever beam vibration technique. Genç et al. [11] handled the modal parameters of cross-laminated timber beams exposed to successive damage.

Ambient vibration test (AVT) is widely utilized as a non-destructive technique for identifying the modal parameters of structures under operational conditions. In AVTs, sensors are strategically placed at nodal points determined from the FE analysis, enabling the acquisition of vibration signals. These collected signals are then processed to identify modal parameters. Therefore, sensor layout has a critical influence on the fidelity of the collected vibration signals, the resolution of modal peaks, and the suppression of redundant or low-signal data [12-14]. On the other hand, the need for numerous sensors in civil engineering structures significantly increases the cost of vibration tests. Thus, it is necessary to select optimal sensor placements (OSP) to both minimize measurement costs and accurately identify modal parameters.

Determination of OSP is an important research topic for many structures, as it directly impacts the efficiency and accuracy of vibration testing conducted for topics such as structural health monitoring, damage detection, and modal parameter identification. A variety of methods have been presented by researchers for this purpose, such as the Effective Independence Method [15], Optimal and Non-Optimal Driving Point Methods [16], Effective Independence Driving Point Residue Method [17], and Sensor Set Expansion Technique [18]. Various studies in the literature have addressed the OSP problem in a wide variety of structural systems such as buildings [19-21], bridges [22-25], and dams [26,27]. However, a few studies have been performed on OSP for composite elements, which have an important place in civil engineering structures. Dinh-Cong et al. [28] proposed a method for OSP and damage detection in laminated composite structures. For this purpose, two numerical models, including a three-layer cross-ply rectangular beam and a four-layer laminated composite plate, were used. Sunca et al. [29] conducted numerical and experimental studies to determine the optimal sensor layout for AVTs of laminated composite and steel cantilever beams. Ručevskis et al. [30] studied the OSP problem for a composite plate with simulated internal damage. An et al. [31] proposed an OSP approach for vibration-based damage detection in composite structures. Moreover, most of these studies were based on numerical models, with limited research addressing the problem through experimental studies. Due to this gap in literature, studies were carried out on determining the OSP for defining the modal parameters by AVTs on steel-timber composite (STC) beams, in this study. To this aim, an STC cantilever beam was constructed, and AVTs were performed to determine its modal parameters. Initially, AVTs of the STC beam were performed using a large number of accelerometers. Subsequently, the optimal sensor layout was determined using the Effective Independence (EFI) method, and the AVTs were repeated accordingly. The suitability of the selected sensor locations in the STC beams was evaluated by comparing the results obtained from both test setups.

2. Effective independence method

Identifying OSP is a critical aspect of vibration tests, as it directly affects the quality of extracted modal information and overall test efficiency. For this purpose, a variety of methods have been proposed by researchers. In this study, the EFI method was used to determine the optimal sensor layout of the STC cantilever beam. This method has been widely applied in OSP of engineering structures and is recognized for its reliability and computational efficiency.

The EFI method aims to maximize the linear independence of selected mode shapes by evaluating candidate sensor locations. Sensor locations that increase the linear independence of the target mode shape matrix are considered for OSP, while those providing the minimal contribution are iteratively eliminated from the candidate set. This selection continues until the desired number of sensors has been reached, ensuring optimal placement for accurate dynamic characterization. The EFI method selects optimal sensor locations based on the contribution of each candidate point, quantified by the Effective Independence (ED)

vector. The ED values of each candidate point are calculated by Eq. (1). In Eq. (1), ψ and λ denote eigenvectors and eigenvalues, respectively. The ED can also be identified from the eigenvectors and expressed by Eq. (2).

$$E_D = [\Phi \psi] \otimes [\Phi \psi] \lambda^{-1} \tag{1}$$

$$E_D = \Phi[\Phi^T \Phi]^{-1} \Phi^T \tag{2}$$

During the OSP selection process, calculated ED values are initially ranked for candidate points, and the smallest is removed. The coefficients are then recalculated using the updated mode shape matrix. This elimination continues iteratively until the target number of sensors has been achieved.

3. Experimental program

3.1. Details of the STC beam

The geometric details of the cantilever STC beam constructed under laboratory conditions are presented in Fig. 1. The specimen comprises four main components: a cross-laminated timber (CLT) panel, a steel profile, screw-type shear connectors, and a support plate. An IPE120 steel profile was used in the STC beam. The steel grade was S235, with nominal yield and ultimate strengths of 235 MPa and 360 MPa, respectively. The CLT panel used in the specimen consisted of three layers of Scotch pine lumber and had dimensions of 75mm in thickness, 300 mm in width, and 1500 mm in length. Each piece of cut lumber was arranged to form the layers of the panel, and the adhesive was applied to ensure bonding between the layers. To ensure adequate adhesion between the layers, KLEIBERIT PUR Adhesive 506.0, a single-component, polyurethane-based, moisture-curing adhesive classified as D4 according to the DIN/EN 204 standard, was applied. Following the application of the adhesive, the three-layer CLT panel was pressed using an industrial-scale hydraulic press capable of applying pressure in both vertical and horizontal directions.

The steel profile and the CLT panel were connected using screw shear connectors spaced at 150 mm intervals. Then, the beam was welded to a 30 mm-thick steel support plate, which was rigidly anchored to a reaction wall. The experimental setup is illustrated in Fig. 2

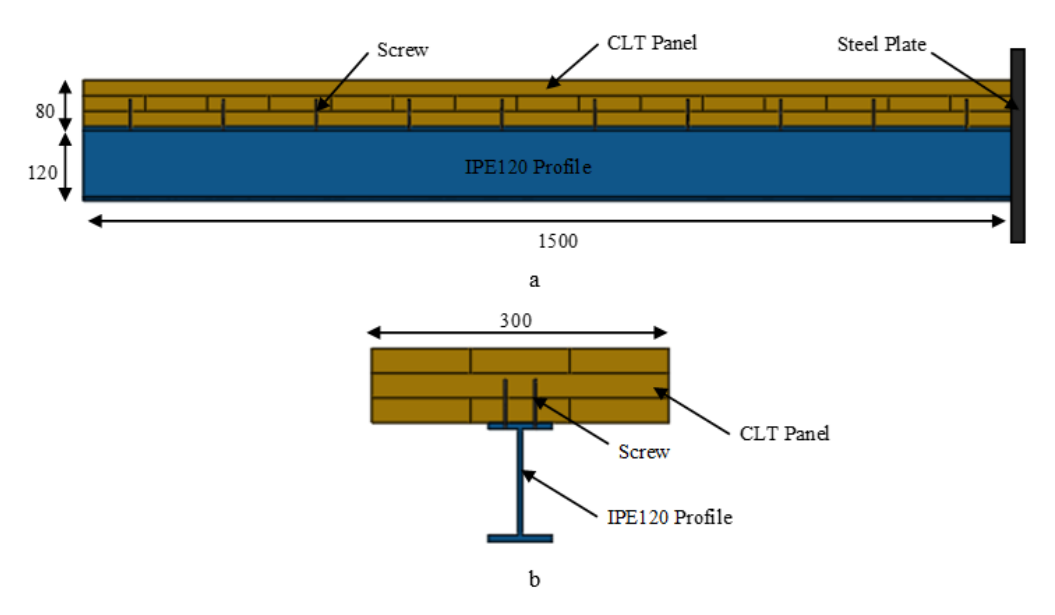


Fig. 1. The geometric details of the cantilever STC beam (a) Plan view, (b) Cross section (amplified)



Fig. 2. Some photos of the test specimen

3.2. Finite element modelling

Prior to the AVTs, an FE model of the test specimen was developed using the SAP2000 program [32]. This initial FE model served two main purposes: to select the potential sensor locations and measurement parameters to be used during AVTs, and to generate the dataset required for determining the optimal sensor layout using the EFI method. In the FE model, the IPE120 steel profile was modeled with elastic beam elements having six degrees of freedom, and the CLT panel was represented by solid elements. The elasticity modulus, Poisson's ratio, and density of the steel were considered as $2.1 \times 108 \text{ kN/m}^2$, 0.3, and 76.97 kN/m^3 , respectively. For the CLT panel, the orthotropic material properties were used. Elastic modulus parallel to grain and perpendicular to grain were taken as $10 \times 106 \text{ kN/m}^2$ and $3.3 \times 105 \text{ kN/m}^2$, respectively. The density of the timber was 4.02 kN/m^3 . The FE model of the STC beam and the first three natural frequencies and corresponding mode shapes are presented in Fig. 3. As shown in Fig. 3, the first three natural frequencies were identified as 46.39 Hz, 245.71 Hz, and 413.02 Hz, respectively.

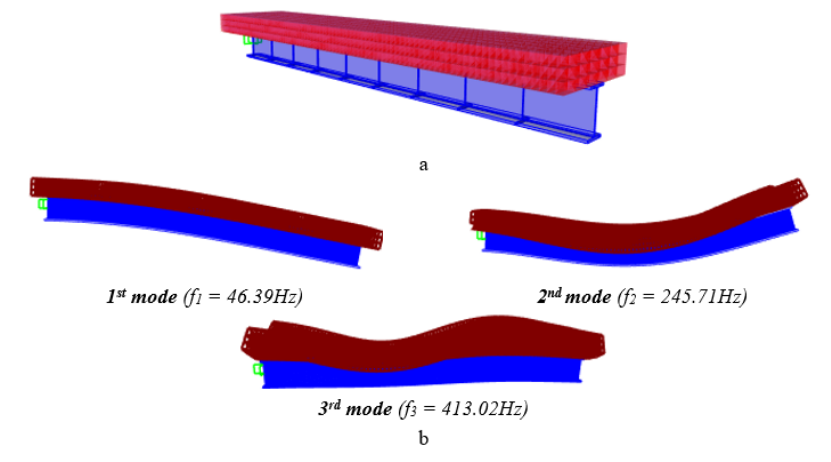


Fig. 3. FE model and modal analysis results of the STC beam (a) FE model of the STC beam, (b) Numerical natural frequencies and related mode shapes

3.3. Ambient vibration test

To identify the modal parameters of the STC beam, AVTs were carried out under operational conditions. A comprehensive experimental campaign with multiple sensors was initially conducted to enable a detailed evaluation of the specimen's response. The vibration test setup included ten B&K 4507-B-005 uniaxial accelerometers (± 7g capacity, frequency range of 0.4–6000 Hz), a 12-channel B&K 3560 data acquisition system, and connecting cables. The collected datasets were imported and analyzed using two software platforms: BK Connect [33] and Pulse [34].

AVT was carried out for a duration of 20 minutes on the STC beam to capture the modal parameters. The frequency range was set to 0–1024 Hz. Data acquisition was carried out using FFT analyzers with a resolution of 800 lines and 100 averages, and a multi-buffer setting of 50 size / 500 ms update rate was applied. Following the vibration tests, the modal parameters of the test specimen were extracted using the Enhanced Frequency Domain Decomposition (EFDD) method. The EFDD method builds upon the classical Frequency Domain Decomposition (FDD) approach by extending its capabilities. In EFDD, the modes are obtained by selecting the peaks in the singular value decomposition graphs calculated from the spectral density function of the response. Due to its ability to estimate damping ratios, unlike the FDD method, and its accuracy in identifying natural frequencies and mode shapes, the EFDD method has been widely used for system identification of several structures. Further details can be found in the relevant literature [35,36]. Fig. 4 illustrates the sensor layout and measurement setup used during the initial AVTs of the STC beam.

Fig. 5 presents the singular values of the spectral density matrices, derived using the EFDD method for identifying the first three natural frequencies and corresponding mode shapes of the STC beam. Moreover, the experimental natural frequencies and the first three mode shapes are also shown in Fig. 5. The first three natural frequencies of the STC beam without OSP were identified as 38.08 Hz, 262.48 Hz, and 614.32 Hz, respectively.

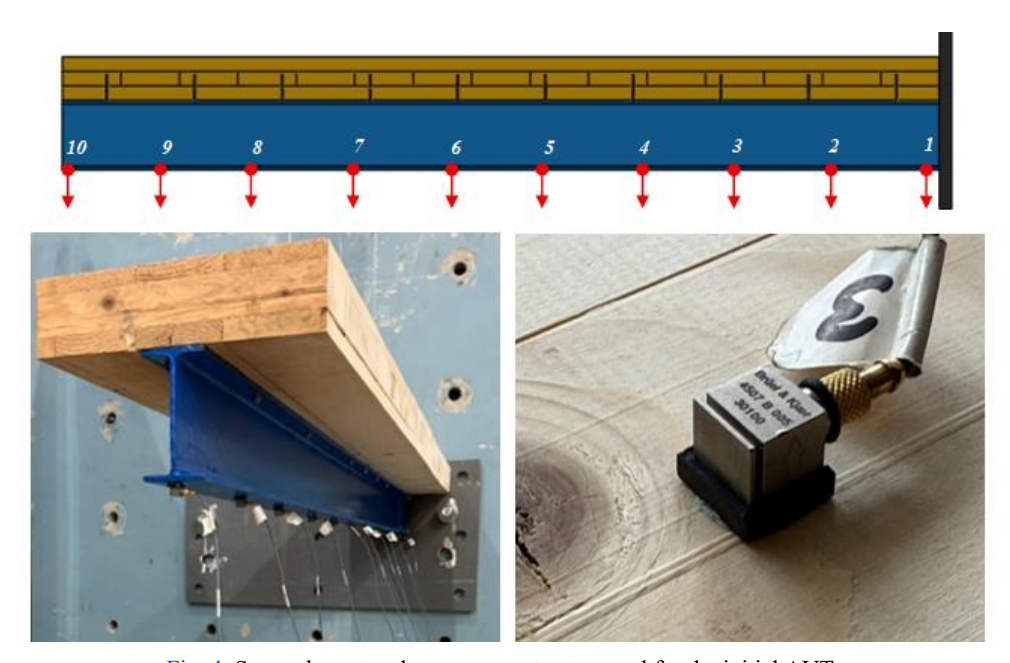


Fig. 4. Sensor layout and measurement setup used for the initial AVTs

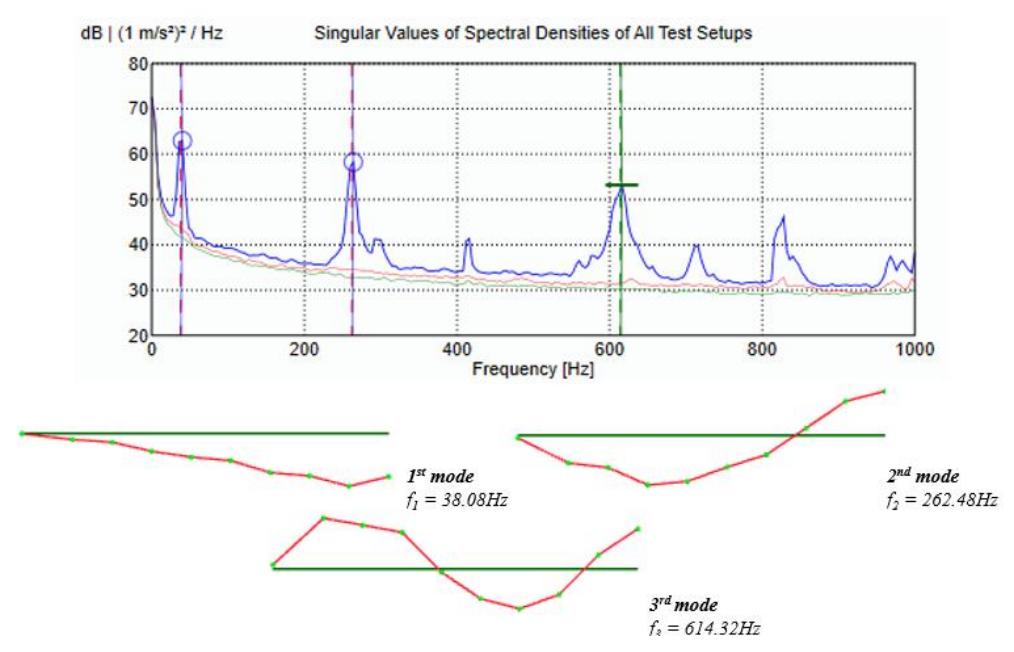


Fig. 5. EFDD result and mode shapes of the STC beam obtained without applying OSP

4. Selection of optimal sensor layout

The OSP for the STC cantilever beam was determined based on target-mode shape matrices, which were obtained from the initial FE model developed in the SAP2000 program. Since AVTs were conducted using ten accelerometers, these locations were also considered as active nodes in the selection of the optimal sensor layout of the beam, and the first three mode shapes were selected as the target modes. The EFI method was employed to identify optimal locations, and in this process, the goal was to use three sensors. Fig. 6 presents a flowchart summarizing the steps involved in the OSP process of the STC beam.

The variation of the effective independence vector distribution obtained for the selected candidate nodes in the final iteration is illustrated in Fig. 7. Through the iterative process conducted until the target number of sensors was reached, the highest effective independence vector values were determined to be 1.00, 0.349, and 0.340, respectively. As shown in Fig. 7, the sensor locations that maximize the linear independence of the selected mode shapes for the desired three-sensor configuration were identified as nodes 3, 9, and 10. Fig. 8 illustrates the optimal sensor layout of the STC beam determined using the EFI method.

AVTs on the STC beam were repeated using the selected optimal sensor configuration. Fig. 9 presents the singular values of spectral density matrices data sets derived using the EFDD method for identifying the first three natural frequencies and corresponding mode shapes of the STC beam after the OSP procedure. Moreover, the experimental natural frequencies and the first three mode shapes are also shown in Fig. 9. The first three natural frequencies of the STC beam with OSP were identified as 38.09Hz, 262.45Hz, and 614.11Hz, respectively. As shown in Fig. 9, the selected configuration of three sensors was sufficient to capture the first two mode shapes; however, the third mode could not be accurately identified. To enable the identification of the third mode shape, AVTs were repeated using four accelerometers, including node 3 of the STC beam, which contributed most significantly to the linear independence of the mode shape matrix after nodes 6, 9, and 10. As a result, the natural frequencies were determined to be 38.08Hz, 262.47Hz, and 614.29Hz. The corresponding EFDD graphs and identified mode shapes from this measurement configuration are presented in Fig. 10. As a result of the vibration tests conducted with four accelerometers, three vertical modes of the STC beam were identified.

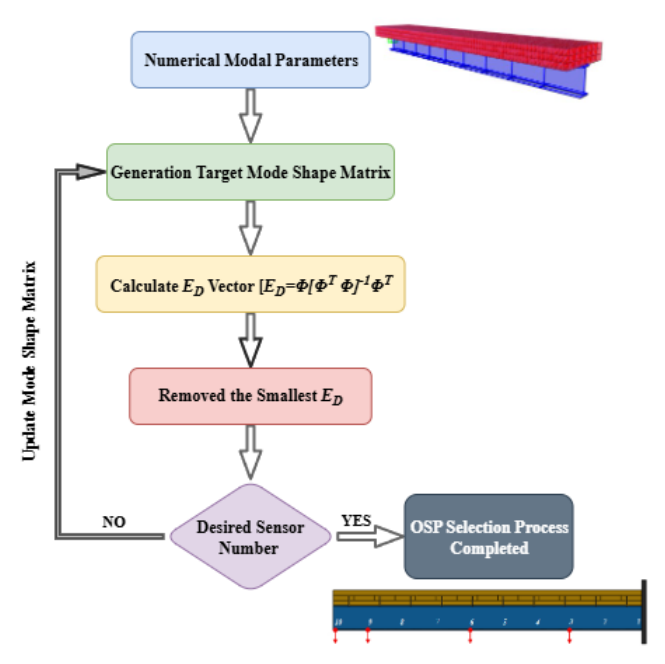


Fig. 6. A flowchart of the OSP selection process of the STC beam

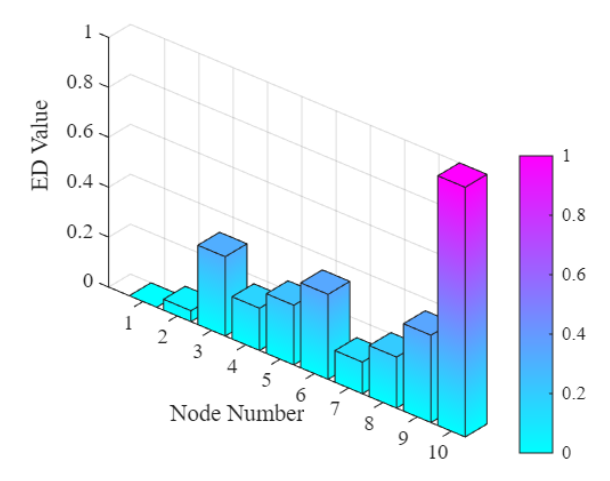


Fig. 7. The variation of the effective independence vector distribution for three desired numbers of sensors

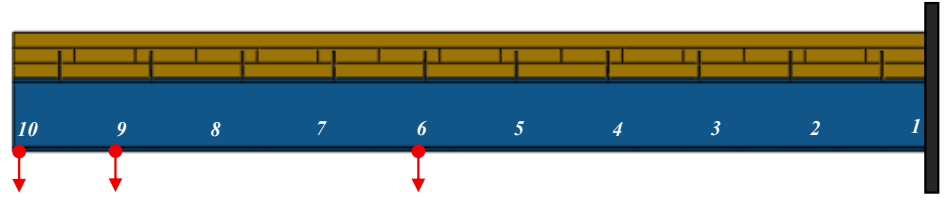


Fig. 8. OSP for the STC beam identified using the EFI method

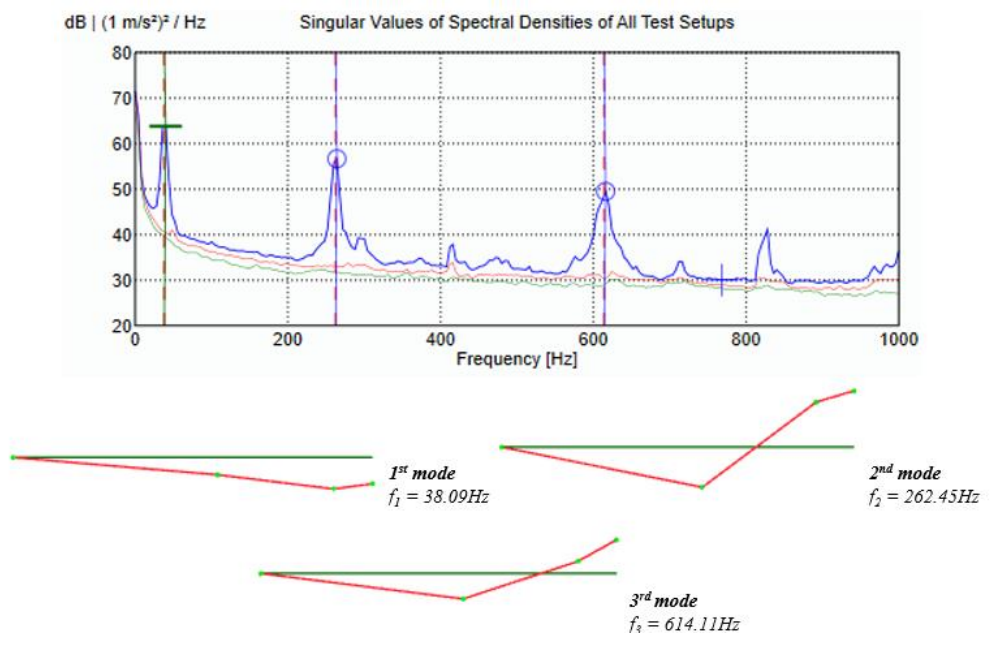


Fig. 9. EFDD results and mode shapes of the STC beam obtained using the three optimal sensor locations

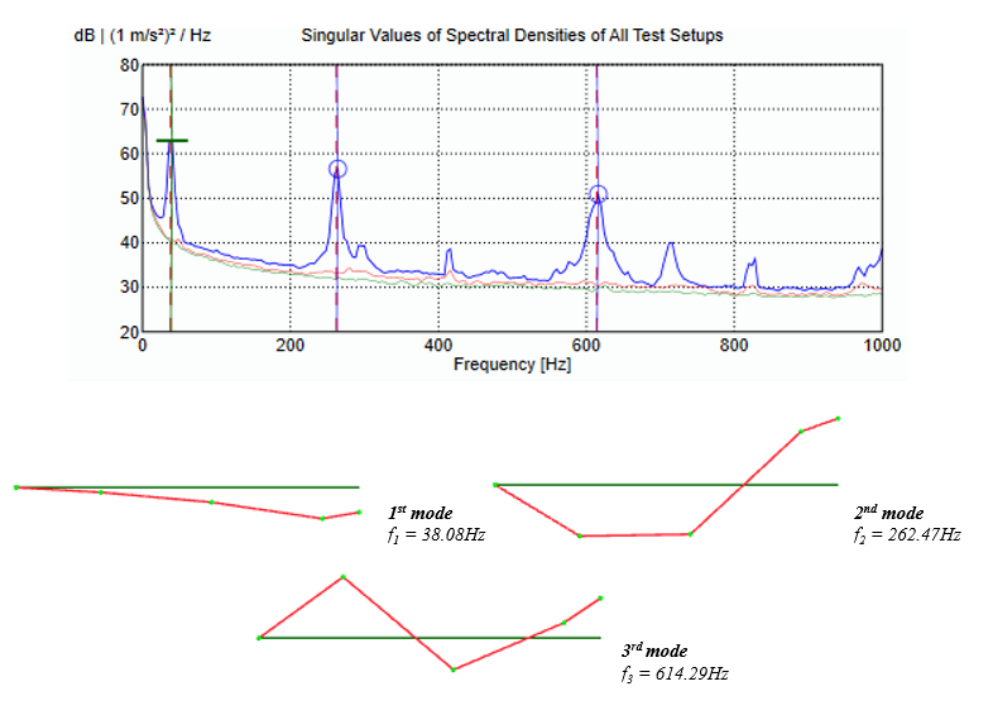


Fig. 10. EFDD results and mode shapes of the STC beam obtained using the four optimal sensor locations

Table 1. Comparisons of modal parameters obtained with and without the application of OSP					
	Without OSP	Diff	With OSP	Diff.	Without OSP
	(three accelerometers)	(%)		(%)	(four accelerometers)
		_		_	
		_		_	
	$f_I = 38.09Hz$	0.026	$f_I = 38.08Hz$	0.000	$f_I = 38.08Hz$
		_			
		_			
	$f_2 = 262.45Hz$	0.011	$f_2 = 262.48Hz$	0.004	$f_2 = 262.47Hz$
		_		_	
	$f_3 = 614.11Hz$	0.034	$f_3 = 614.32Hz$	0.005	$f_3 = 614.29Hz$

Table 1. Comparisons of modal parameters obtained with and without the application of OSP

As observed, the natural frequencies obtained with and without OSP were remarkably similar. Table 1 presents the natural frequencies obtained with and without the application of OSP. The comparative analysis revealed that the natural frequencies obtained with and without OSP were nearly identical, demonstrating that a reduced number of sensors can reliably capture the global dynamic characteristics of the STC beams. When using three sensors, the differences between the frequencies obtained with OSP and those obtained without OSP were approximately 0.026%, 0.011%, and 0.034%, respectively. For the tests conducted with four sensors, these differences were calculated as 0.00%, 0.004%, and 0.005%, respectively. Similar observations were reported by Sunca et al. [29] for laminated composite and steel beams, suggesting that the EFI-based OSP strategy is robust across different composite configurations. However, while the first two mode shapes were captured with fidelity using three sensors, the third mode could not be identified accurately (Fig. 9). In AVT, where local modes are not important, the number and placement of accelerometers generally have a minimal influence on the identification of natural frequencies. While a single accelerometer placed anywhere on the structure may be sufficient to extract basic modal parameters such as natural frequencies and damping ratios, obtaining accurate mode shapes requires careful consideration of both the number and positions of sensors. From a practical standpoint, the ability to reduce instrumentation without sacrificing accuracy has significant implications for large-scale structural health monitoring, where cost and accessibility are critical considerations. Nonetheless, the sharper but less detailed mode shapes obtained with fewer sensors may pose challenges for damage localization or high-resolution monitoring tasks.

5. Conclusions

In this study, the applicability and effectiveness of the OSP strategy for modal parameter identification of an STC cantilever beam were investigated through AVT. For this purpose, an STC beam was fabricated under laboratory conditions. AVTs were conducted using both an initial dense sensor configuration and an optimized sensor layout determined via the EFI method. To extract the modal parameters of the STC beam, the EFDD method in the frequency domain was applied. A comparative evaluation was carried out between the modal parameters obtained before and after the application of the OSP procedure. Based on the results, the following conclusions can be drawn:

1. The first three experimental natural frequencies of the STC beam were identified in the range of 38.09-614.32 Hz under the initial sensor configuration, while frequencies in the range of 38.09-614.11 Hz were obtained following the OSP procedure using three accelerometers.

2. The selected configuration of three sensors was sufficient to capture the first two mode shapes; however, the third mode could not be accurately identified. Therefore, AVTs were repeated using four accelerometers to enable the identification of the third mode shape. The vibration tests conducted with the optimal placement of four accelerometers yielded natural frequencies in the range of 38.08 Hz and 614.29 Hz.

- 3. When using three sensors, the differences between the frequencies obtained with OSP and those obtained without OSP were approximately 0.026%, 0.011%, and 0.034%, respectively. For the tests conducted with four sensors, these differences were calculated as 0.00%, 0.004%, and 0.005%, respectively.
- 4. The first three mode shapes of the STC beam obtained under both the initial sensor configuration and after the application of the OSP procedure were found to be consistent. While the mode shapes remained consistent across different sensor configurations, the reduced number of sensors resulted in sharper representations of the mode shapes.
- 5. The findings demonstrated that the EFI method was effective for the STC beam, enabling accurate representation of the structural behavior using a limited number of accelerometers.

Although the findings demonstrated the effectiveness of the EFI-based OSP procedure for steel-timber composite beams under laboratory conditions, several limitations should be acknowledged. First, the scalability of the proposed approach to larger and more complex structures composed of this type of composite element (e.g., bridges, multi-story buildings) remains uncertain and requires further validation. Second, while AVTs in laboratory settings benefited from a controlled environment, the influence of measurement noise and environmental disturbances in real-world applications could reduce the accuracy of the identified modal parameters, particularly for higher or closely spaced modes. Finally, the applicability of the method to in-situ conditions may be constrained by boundary condition uncertainties, accessibility issues, and sensor installation challenges, which were not captured in the present experimental setup.

In light of these limitations, several directions for future research can be suggested. Extending the methodology to different loading and operational conditions (e.g., varying temperature, humidity, or live load scenarios) would provide a more comprehensive assessment of its robustness. Furthermore, combining the OSP strategy with vibration-based damage detection techniques could enhance its potential for structural health monitoring, especially in applications where early identification of local damage is critical. Investigations on full-scale structures and long-term monitoring campaigns would also contribute to bridging the gap between laboratory validation and real-world implementation.

Declaration of conflicting interests

The author(s) declared no potential conflicts of interest with respect to the research, authorship, and/or publication of this article.

Funding

No funding was received for this study.

Data availability statement

The datasets generated and/or analyzed during the current study are available from the corresponding author on reasonable request.

References

- [1] Altunişik AC, Öztürk MM, Genç AF, Kaya A, Akbulut YE, Sunca F, Günaydin M (2025) Estimating fundamental frequency of masonry arches under elevated temperature: Numerical analysis and validation using ambient vibration tests. Arch Civ Mech Eng 25(23):1–32.
- [2] Okur FY (2025) Towards a digital twin approach for structural stiffness assessment: A case study on the Cho'ponota L1 Bridge. Appl Sci 15(12):6854.
- [3] Zini G, Giachetti A, Betti M, Bartoli G (2024) Vibration signature effects on damping identification of a RC bridge under ambient vibrations. Eng Struct 298:116934.
- [4] Chioccarelli E, Giunta D, De Angelis A, Bilotta A (2024) Discussing optimal sensor placement for ambient vibration test of an existing bridge. Eng Struct 310:118000.
- [5] Zhou Y, Liu Y, Lian Y, Pan T, Zheng Y, Zhou Y (2025) Ambient vibration measurement-aided multi-1D CNNs ensemble for damage localization framework: Demonstration on a large-scale RC pedestrian bridge. Mech Syst Signal Process 224:111937.
- [6] Wu Y, Kang F, Zhang Y, Li X, Li H (2024) Structural identification of concrete dams with ambient vibration based on surrogate-assisted multi-objective salp swarm algorithm. Struct 60:105956.
- [7] Kalkan Okur E, Okur FY, Sunca F, Günaydin M, Aydoğan D, Altunişik AC (2025) Real-time structural health monitoring of Yusufeli Arch Dam: A detailed analysis of dynamic characteristics during water impoundment. Nondestruct Test Eval 1–27.
- [8] Bernardo VMS, Campos Costa A, Candeias PJD, da Costa AG, Marques AIM, Carvalho AR (2022) Ambient vibration testing and seismic fragility analysis of masonry building aggregates. Bull Earthq Eng 20(10):5047–5071.
- [9] Astroza R, Ebrahimian H, Conte JP, Restrepo JI, Hutchinson TC (2022) Statistical analysis of the modal properties of a seismically-damaged five-story RC building identified using ambient vibration data. J Build Eng 52:104411.
- [10] Wang Z, Li L, Gong M (2012) Measurement of dynamic modulus of elasticity and damping ratio of wood-based composites using the cantilever beam vibration technique. Constr Build Mater 28(1):831–834.
- [11] Genç AF, Kahya V, Altunışık AC, Günaydın M, Demirkır C (2021) Assessment of modal characteristics of cross-laminated timber beams subject to successive damages. Arch Civ Mech Eng 21(3):128.
- [12] Chang M, Pakzad SN (2014) Optimal sensor placement for modal identification of bridge systems considering number of sensing nodes. J Bridge Eng 19(6):04014019.
- [13] Jung BK, Cho JR, Jeong WB (2015) Sensor placement optimization for structural modal identification of flexible structures using genetic algorithm. J Mech Sci Technol 29:2775–2783.
- [14] Altunisik AC, Sevim B, Sunca F, Okur FY (2021) Optimal sensor placements for system identification of concrete arch dams. Adv Concr Constr 11(5):397–407.
- [15] Kammer DC (1991) Sensor placement for on-orbit modal identification and correlation of large space structures. J Guid Control Dyn 14(2):251–259.
- [16] Imamovic N (1998) Model validation of large finite element model using test data. PhD Thesis, Imperial College, London, UK.
- [17] Kim HB, Park YS (1997) Sensor placement guide for structural joint stiffness model improvement. Mech Syst Signal Process 11(5):651–672.
- [18] Kammer DC (2005) Sensor set expansion for modal vibration testing. Mech Syst Signal Process 19(4):700–713.
- [19] Bakir PG (2011) Evaluation of optimal sensor placement techniques for parameter identification in buildings. Math Comput Appl 16(2):456–466.
- [20] Chaves E, Barontini A, Mendes N, Compán V, Lourenço PB (2023) Methodologies and challenges for optimal sensor placement in historical masonry buildings. Sensors 23(23):9304.
- [21] Saeed S, Sajid SH, Chouinard L (2024) Optimal sensor placement for enhanced efficiency in structural health monitoring of medium-rise buildings. Sensors 24(17):5687.
- [22] Li DS, Li HN, Fritzen CP (2007) The connection between effective independence and modal kinetic energy methods for sensor placement. J Sound Vib 305(4–5):945–955.
- [23] Pachón P, Castro R, García-Macías E, Compan V, Puertas E (2018) E. Torroja's bridge: Tailored experimental setup for SHM of a historical bridge with a reduced number of sensors. Eng Struct 162:11–21.
- [24] Chai W, Yang Y, Yu H, Yang F, Yang Z (2022) Optimal sensor placement of bridge structure based on sensitivity-effective independence method. IET Circuits Devices Syst 16(2):125–135.

[25] Gonen S, Demirlioglu K, Erduran E (2023) Optimal sensor placement for structural parameter identification of bridges with modeling uncertainties. Eng Struct 292:116561.

- [26] He L, Lian J, Ma B, Wang H (2014) Optimal multiaxial sensor placement for modal identification of large structures. Struct Control Health Monit 21(1):61–79.
- [27] Zhu K, Gu C, Qiu J, Liu W, Fang C, Li B (2016) Determining the optimal placement of sensors on a concrete arch dam using a quantum genetic algorithm. J Sensors 2016(1):2567305.
- [28] Dinh-Cong D, Dang-Trung H, Nguyen-Thoi T (2018) An efficient approach for optimal sensor placement and damage identification in laminated composite structures. Adv Eng Softw 119:48–59.
- [29] Sunca F, Okur FY, Altunişik AC, Kahya V (2021) Optimal sensor placement for laminated composite and steel cantilever beams by the effective independence method. Struct Eng Int 31(1):85–92.
- [30] Ručevskis S, Rogala T, Katunin A (2022) Optimal sensor placement for modal-based health monitoring of a composite structure. Sensors 22(10):3867.
- [31] An H, Youn BD, Kim HS (2022) A methodology for sensor number and placement optimization for vibration-based damage detection of composite structures under model uncertainty. Compos Struct 279:114863.
- [32] SAP2000 (2015) Structural analysis program. Computers and Structures Inc., Berkeley, CA.
- [33] BK Connect (2023) BK Connect software. Bruel and Kjaer, Sound and Vibration Measurement A/S, Nærum, Denmark.
- [34] Pulse (2023) Pulse software. Bruel and Kjaer, Sound and Vibration Measurement A/S, Nærum, Denmark.
- [35] Bendat JS, Piersol AG (2011) Random data: Analysis and measurement procedures. John Wiley & Sons, Hoboken.
- [36] Brincker R, Zhang L, Andersen P (2000) Modal identification from ambient responses using frequency domain decomposition. In: Proc. IMAC 18: Int Modal Analysis Conf, San Antonio, USA, 7–10 Feb 2000, pp. 625–630.